



**HAL**  
open science

## On the confinement parameter in HRAM bubble Rayleigh-Plesset modelling

T. Fourest, E. Deletombe, J. Dupas, M. Arrigoni, Jean-Marc Laurens

### ► To cite this version:

T. Fourest, E. Deletombe, J. Dupas, M. Arrigoni, Jean-Marc Laurens. On the confinement parameter in HRAM bubble Rayleigh-Plesset modelling. 13th International Conference on Structures Under Shock and Impact (SUSI 2014), Jun 2014, NEW FOREST, United Kingdom. hal-01071623

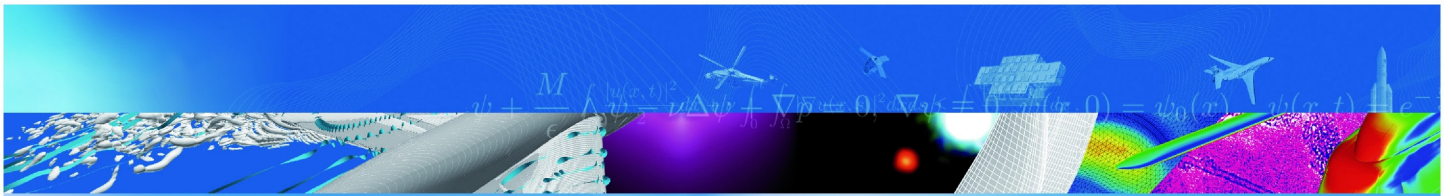
**HAL Id: hal-01071623**

**<https://onera.hal.science/hal-01071623>**

Submitted on 6 Oct 2014

**HAL** is a multi-disciplinary open access archive for the deposit and dissemination of scientific research documents, whether they are published or not. The documents may come from teaching and research institutions in France or abroad, or from public or private research centers.

L'archive ouverte pluridisciplinaire **HAL**, est destinée au dépôt et à la diffusion de documents scientifiques de niveau recherche, publiés ou non, émanant des établissements d'enseignement et de recherche français ou étrangers, des laboratoires publics ou privés.



T I R É À P A R T

## **On the confinement parameter in HRAM bubble Rayleigh-Plesset modelling.**

T. Fourest, E. Deletombe, J. Dupas,  
M. Arrigoni \*, J.M. Laurens \*

13th International Conference on Structures  
Under Shock and Impact (SUSI 2014)  
NEW FOREST, GRANDE BRETAGNE  
3-5 juin 2014

TP 2014-579

**ONERA**

THE FRENCH AEROSPACE LAB

r e t o u r   s u r   i n n o v a t i o n



On the confinement parameter in HRAM bubble Rayleigh-Plesset modelling.

*Sur le paramètre de confinement dans les modélisations de type Rayleigh-Plesset des bulles  
créées lors de coups de bélier hydrodynamiques.*

par

T. Fourest, E. Deletombe, J. Dupas, M. Arrigoni \*, J.M. Laurens \*

\* ENSTA-Bretagne/LBMS

**Résumé traduit :**

La conception de réservoirs de carburant au regard des pressions générées par des phénomènes de coup de bélier hydrodynamique est un besoin majeur pour les avions Civils et Militaires, afin de réduire leurs vulnérabilités. Des similarités dans le comportement des bulles entre le coup de bélier hydrodynamique et les explosions sous-marines ont été observées dans des essais récents de pénétration / entrée dans l'eau de projectiles hautes vitesses. Les travaux présentés concernent l'application de l'équation de Rayleigh-Plesset - classiquement utilisée pour l'analyse de la dynamique d'une bulle (incluant les explosions sous-marines) - aux bulles créées par des coups de bélier hydrodynamique induits par la pénétration de projectiles balistiques dans une géométrie confinée remplie d'un liquide. L'équation de Rayleigh-Plesset est appliquée à deux cas d'impacts, un dans un réservoir de dimensions restreintes, fermé et un dans une piscine hydrodynamique de plus grandes dimensions. L'initialisation du modèle est basée sur des données expérimentales et sur le principe de conservation de l'énergie cinétique initiale du projectile. Pour appliquer cette équation une relation entre les pressions appliquées à la structure et les déformations de la structure est nécessaire. Cependant cette relation ne peut être obtenue explicitement que pour des réservoirs sphériques. Les auteurs discutent sur les paramètres de cette équation et comparent leurs valeurs calibrées avec celles obtenues avec des formules analytiques.



# On the confinement parameter in HRAM bubble Rayleigh-Plesset modelling

T. Fourest<sup>1</sup>, E. Deletombe<sup>1</sup>, J. Dupas<sup>1</sup>, M. Arrigoni<sup>2</sup>, J-M Laurens<sup>2</sup>

<sup>1</sup> *ONERA - The French Aerospace Lab*

<sup>2</sup> *ENSTA Bretagne, Lab Brestois de Mécanique et des Systèmes*

## Abstract

The design of fuel tanks with respect to Hydrodynamic Ram (HRAM) pressure is a major need for Civil and Military aircraft in order to reduce their vulnerability. Similarities in bubble behaviour between HRAM and underwater explosion situations were observed in recent high-speed tank penetration/water entry experiments. The present work concerns the application of a confined version of the Rayleigh-Plesset equation - which is classically used for bubble dynamics analysis (including underwater explosion) - to simulate a bubble created by an HRAM event induced by projectile penetration at ballistic speed in a confined geometry filled with a liquid. This equation is applied to two cases of impact, one in a small closed tank and one in a larger pool. The initialisation of the model is based on experimental data and a conservation principle of the initial energy (of the projectile). To apply this equation a relationship between the pressure applied on the structure and the structure deformation is needed. However it can only be obtained explicitly for spherical containers. The authors discuss on the parameters needed in this equation and compare their calibrated values to theoretical ones calculated with analytical plates formulae.

## 1 Introduction

In the event of impact of high speed/high energy projectiles on liquid filled tanks, the container may suffer large hydrodynamic loads that could possibly rupture the entire structure. This impact scenario is referred as Hydrodynamic Ram (HRAM). The need of tools for physical understanding of the

hydrodynamic effects that occur during a HRAM event is an increasing one as well in the civil domain as for the military aircraft design (vulnerability requirement). Indeed physical understanding of HRAM dynamics would permit to improve structures with respect to this particular threat.

The HRAM event is generally characterized by four phases first described by Ball [2]: the shock phase, the drag phase, the cavity growth and collapse phases. These phases and the associated loads are illustrated in Figure 1.

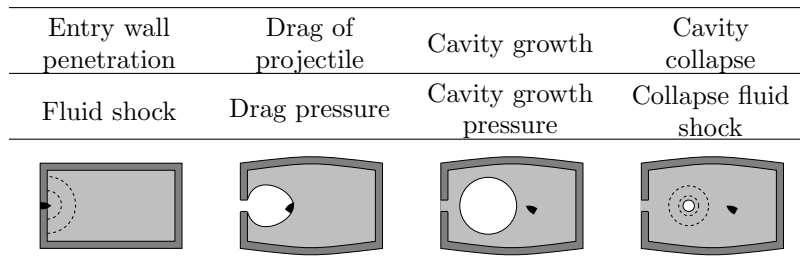


Figure 1: General scenario of Hydrodynamic Ram event in liquid filled tank.

The first experimental observations on the subject were done by McMillen [6] who recorded the shock waves and drag phase produced by the penetration of small steel spheres at high speed ( $610 \text{ m.s}^{-1}$  to  $1500 \text{ m.s}^{-1}$ ) into water by using a shadowgraphs method. He was particularly interested in the shock waves characteristics. He observed that the projectile is quickly slowed down by drag and that the shock wave propagates at the speed of sound in water.

Shi et al.[8] observed the cavity motion induced by a medium speed ( $342 \text{ m.s}^{-1}$ ) water entry of a bullet. More recently Deletombe et al. [5] presented experiments of impact in water of non-academic projectiles (7.62 mm bullet) at ballistic speed ( $850 \text{ m.s}^{-1}$ ). The same phases of water entry occurred during these experiments. They enlightened the effect of the tumbling of projectiles on the cavity shape during HRAM events.

During tumbling the projectile transmits more quickly its momentum to the liquid medium. An extreme case would be an instantaneous transfer that would lead to a spheric cavity bubble. At the opposite, a projectile that cannot tumble will transfer its kinetic energy more slowly and will create a more elongated cavity shape in its wake. Bless [3] observed that the pressure resulting from the tumbling of the projectile could be five times superior to the one observed in a case without tumbling.

Generally, during the water entry of a projectile, the cavity created by the drag of the projectile will be enclosed by the surrounding free surface of the liquid, and a cavity bubble will then be created. After it has completed its growth, this cavity will eventually collapse. Deletombe et al. [4] performed pressure measurements for 7.62 mm bullet impacts on water filled tanks, and observed greater pressures during the drag phase than during the cavity

growth but in shorter time time. They nevertheless concluded that none of these phases could be neglected for the sizing of structures because they both could carry significant impulse.

The present work focuses on the cavity growth and collapse phase in the case of tumbling of projectiles. This case seems to lead to higher pressures. A conservative approach would be to design structures to resist this threat. However tumbling of projectiles is particularly difficult to correctly simulate with current numerical tools. The more advanced numerical simulations of this phenomenon presented in the open literature deal with non-deformable projectiles [11]. These studies either use Lagrange-Euler finite element methods or particle type solutions. Anyway the whole sequence of event up to the collapse (that might take up to 30 ms) is not simulated. Another approach is chosen here, which is to study this complex phenomenon with an analytical tool. Pioneer works on the subject were done by Stepka and Morse [9]. They identified the factors that affect the liquid loading during an HRAM event, tried to analyse the effects of the different parameters on the survivability of tanks, but they could not clearly establish a correlation that could include the effects of all the parameters.

Recent experimental results in particular those presented in [5] permit to observe the evolution of the bubble created in the wake of a tumbling projectile. The bubble dynamics seems to be comparable to bubble dynamics observed in during underwater explosion phenomena [1]. This bubble dynamics is described using a modified version of the Rayleigh-Plesset equation introducing confinement effect of the container on the bubble pulsating. The object of the present work is to discuss on the confinement parameter in this confined version of the classic Rayleigh-Plesset equation for bubble dynamics, that is applied to bubbles created by ballistic impacts.

## 2 Studied cases

The Rayleigh-Plesset approach has been used for two cases : the first one is a 7.62 mm NATO ballistic impact in a generic Airbus-Innovation closed water-filled tank. The second case is a ballistic shot in a large ONERA/DAAP pool. In both cases the impact is normal to the entry wall of the tank or free surface of liquid. These experiments are reported in [5]. These two tests correspond respectively to a confined tank and a larger domain. The pool dimensions are approximately  $22 \times 1.5 \times 1.5 \text{ m}^3$  and the tank dimensions are  $0.3 \times 0.54 \times 0.66 \text{ m}^3$ .

## 3 Confined Rayleigh-Plesset equation

A modification of the classic Rayleigh-Plesset equation is proposed here to account for confinement effects without changing the method of resolution. To obtain this equation and use it to predict HRAM bubble dynamics, a



spherical gas bubble in a spherical finite domain of liquid is first considered, and the following assumptions are made:

- Spherical deformation of the bubble interface;
- Instantaneous energy transfer from kinetic energy of the bullet to the liquid;
- Gravity effects are negligible;
- Idealised case of zero mass transport across the bubble interface is considered,
- Dynamic viscosity and surface tension effects are negligible due to the large dimensions of the bubbles,
- An initial amount of non-condensable gas (here air) is considered, in first approach its behaviour is assumed to be adiabatic.
- The liquid domain is considered to be incompressible and of finite dimensions;
- An elastic structural confinement is added by means of a spherical shell.

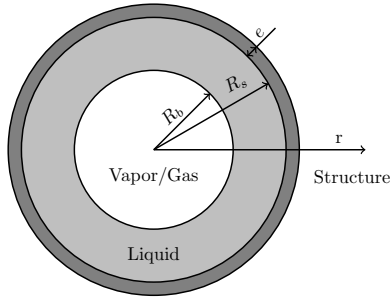


Figure 2: Sketch of the system considered in the proposed confined Rayleigh-Plesset equation.

The equation of mass conservation for a radial movement is expressed in spherical coordinates, it reduces due to the assumptions to (1).

$$r^2 \dot{r} = R_b^2 \dot{R}_b \quad (1)$$

with  $R_b$  the radius of the bubble and  $\dot{r}$  the radial speed of the liquid at radius  $r$ . Using the previous assumptions, the equation of conservation of momentum in the radial direction is reduced to (2).

$$\ddot{r} + \dot{r} \frac{\partial \dot{r}}{\partial r} + \frac{1}{\rho} \frac{\partial P}{\partial r} = 0 \quad (2)$$

It is considered that the centre of the bubble corresponds to the centre of the container. The initial external radii  $R_{s_0}$  of the liquid domains were defined as the radii that yield the same volume as the tested containers (respectively  $50 \text{ m}^3$  for the pool and  $7.7 \cdot 10^{-2} \text{ m}^3$  for the tank). The behaviour

of the liquid is assumed to be incompressible, hence the current radius of the elastic sphere  $R_s$  is related to the radius of the bubble (3):

$$R_s = (R_{s_0}^3 + R_b^3 - R_{b_0}^3)^{1/3} \quad (3)$$

Integrating (2) between  $R_s$  and  $R_b$ , using (1) and defining  $\Lambda = R_b/R_s$ , the same equation as in [7] is found (4):

$$R_b \ddot{R}_b + \frac{3}{2} \dot{R}_b^2 + \frac{P_s(t) - P_b(t)}{\rho} - 2 \dot{R}_b^2 \Lambda - R_b \ddot{R}_b \Lambda + \frac{1}{2} \dot{R}_b^2 \Lambda^4 = 0 \quad (4)$$

with  $P_s$  the pressure at the interface between the liquid and the structural sphere.  $\Lambda$  is then defining a geometrical parameter with respect to the finite size of the considered fluid domains.

A similar equation to the Rayleigh-Plesset equation is obtained with the addition of three terms that vanish when  $R_s = \infty$  (infinite medium)).

Another relation between the pressure applied on the wall and the structural sphere response is needed. If the containers behaviour is assumed elastic and linear, a good approximation of the relationship is obtained by assuming proportionality between the variation of pressure on the sphere wall  $P_s - P_{s_0}$  and the variation of the internal volume of the sphere  $V - V_0$ . This coefficient of proportionality will be hereafter called confinement parameter, and denoted  $\alpha$  in (5).

$$P_s - P_{s_0} = \alpha \cdot (V - V_0) \quad (5)$$

#### 4 Application of confined Rayleigh-Plesset equation for bubble created by HRAM events

The initial conditions of the Rayleigh-Plesset equation determined from the ONERA experiments are linked to the initial time chosen for the analysis (when a bubble cavity reasonably appears). To choose the starting times for Rayleigh-Plesset simulations, energetic considerations are used e.g. when the liquid initial kinetic energy in Rayleigh-Plesset equation is equal to the theoretical initial kinetic energy of the projectile that created the bubble (approximately 3.5 kJ in the pool and 2.9 kJ in the tank). It has been observed that it corresponded approximately to the beginning of the growth stage of the bubble cavity in the tests. As the energetic partition between the kinetic energy transferred to the liquid and the energy dissipated by the deformation of the projectile is not known, no dissipative phenomena are considered here: the whole projectile kinetic energy is assumed to be transferred to the liquid. The amount of kinetic energy of the liquid is calculated using the assumption of incompressibility of the liquid (6):

$$E_k = 2\pi\rho R_b^4 \dot{R}_b^2 \left( \frac{1}{R_b} - \frac{1}{R_s} \right) \quad (6)$$

#### 4.1 Experimental calibration of $\alpha$

First, before searching to obtain the numerical values of  $\alpha$  from analytical formulae, its values are obtained by calibration using the experimental results. These values are denoted  $\alpha_{calib}$ .

The modified Rayleigh-Plesset equation is solved with a Runge-Kutta fourth order method. The coefficients  $\alpha_{calib}$  have been chosen to obtain good agreement in amplitude between the experimental radius and those obtained numerically (see Figure 3). Table 1 summarises the initial conditions used for these simulations.  $\alpha_{calib} = 1.5 \text{ MPa}\cdot\text{mm}^{-3}$  and  $\alpha_{calib} = 150 \text{ MPa}\cdot\text{mm}^{-3}$  for the pool and tank respectively.

Table 1: Numerical values of the initial conditions used for each case in confined Rayleigh-Plesset simulations.

Case	$P_{b_0}$ (MPa)	$t_0$ (ms)	$R_{b_0}$ (mm)	$\dot{R}_{b_0}$ (mm.ms <sup>-1</sup> )	$R_{s_0}$ (mm)	$\alpha_{calib}$ (MPa.mm <sup>-3</sup> )
Pool	$8.1\cdot 10^{-3}$	0.5	42.3	86.44	2200	1.5
Tank	$2.23\cdot 10^{-3}$	0.26 ms	48.5	70.6	264	150

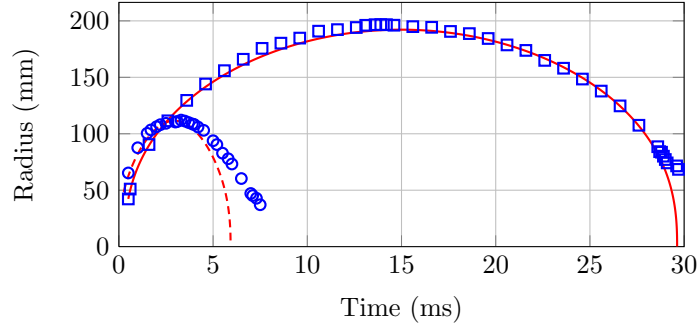


Figure 3: Radius evolution in tank test ( $\circ$ ), pool test ( $\square$ ) and predicted with confined RP in tank ( $---$ ) and pool ( $---$ ) with  $\alpha_{calib}$ .

#### 4.2 Application with elasticity formula for the structure response

The results obtained by calibrating the coefficients  $\alpha$  are found to be quite satisfactory. The extent to which the numerical values of this coefficient can be predicted with analytical formulae will be now investigated.

First the case of an “academic container” is studied. For this a spherical elastic container is used. Obviously this model induces large differences with the real containers. A mono-material spherical shell is used instead of a multi-material parallelepipedic container assembled by metallic bolts. However this model will be used as a reference to compare with more precise modellings later.

#### 4.2.1 Analytical value of $\alpha$ for spherical tanks

In case of a spherical container, the structure can be modelled using the theory of elasticity on a spherical thick shell. The numerical values of the coefficient  $\alpha$  can be determined for this configuration, it will be denoted  $\alpha_s$  in (7):

$$\alpha_s = \frac{E}{4\pi} \cdot \left( \frac{(R_{s_0} + e)^3 - R_{s_0}^3}{R_{s_0}^3} \right) \cdot \left( \frac{2}{2(1 - 2\nu)R_{s_0}^3 + (1 + \nu)(R_{s_0} + e)^3} \right) \quad (7)$$

The confinement parameter obtained by taking into account confinement effect with structure modelled as a mono-material spherical elastic thick shell with materials presented in Tables 2 and 3 is far from the calibrated values.

Table 2: Numerical values used for the calculation of the coefficient  $\alpha_s$  for a  $V = 0.3 \times 0.54 \times 0.66 \text{ m}^3$  tank (see Airbus-Innovation tank).

Tank material	E (MPa)	$\nu$	e (mm)	$\alpha_s$ (MPa.mm <sup>-3</sup> )
OMC <sup>a</sup>	110000	0.3	6	$3.0 \cdot 10^4$
Plexiglass	2600	0.3	40	$5.1 \cdot 10^3$
Steel	210000	0.3	50	$3.4 \cdot 10^5$

<sup>a</sup>Organic Matrix Composite

Table 3: Numerical values used for the calculation of the coefficient  $\alpha_s$  for a  $V = 22 \times 1.5 \times 1.5 \text{ m}^3$  tank (see ONERA DAAP Pool).

Pool material	E (MPa)	$\nu$	e (mm)	$\alpha_s$ (MPa.mm <sup>-3</sup> )
Concrete	30000	0.3	120	3.3
Glass	70000	0.3	40	26
Free surface	–	–	–	–

As expected none of the materials permits to correlate with the experimental results. There is respectively a ratio 30 and 2 between the calibrated values and the best obtained by considering spherical shell that yield the same volume than the tank and the pool. The larger difference in the tank case is probably due to weaker confinement effects induced by the pool than by the tank, due to the large dimensions of the pool and to its free surface.

#### 4.2.2 Application with elastic plates formulae

Indeed in the experiment the containers are not spherical, and are assemblies of several parts with different materials. In this part the numerical values of the coefficient  $\alpha$  is calculated with plates formulae. It will be denoted  $\alpha_{plate}$ . In this part only the tank case is considered as the pool yield a free surface, that cannot be taken into account with this model.

##### 4.2.2.1 Plates formulae to obtain $\Delta V$

The total variation of the container volume is obtained by adding the variation of volume allowed by the deformation of each panel of the tank:  $\Delta V = 2(\Delta V_{plate_{OMC}} + \Delta V_{plate_{Steel}} + \Delta V_{plate_{Plaxi}})$ . The plate are considered to be embedded and submitted to a uniform pressure field.

The variation of volume allowed by a single panel (see fig 5), is calculated using (8).

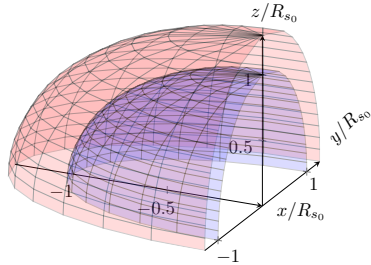


Figure 4: Variation of volume for a quarter of the structural sphere submitted to uniform internal pressure before application of the pressure (blue) and after (red).

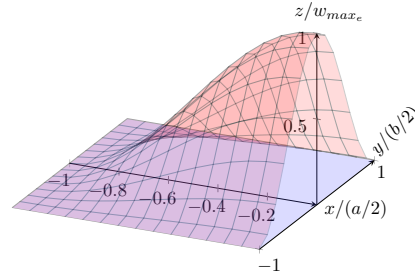


Figure 5: Variation of volume for half of an embedded plate submitted to uniform pressure before application of the pressure (blue) and after (red).

$$\Delta V_{plate} = \iint_S w_{emb} \cdot dS \quad (8)$$

The bending of each plate  $w_{emb}$  is calculated according to Timoshenko [10]:

$$w_{emb} = w_{ss} + w_1 + w_2 \quad (9)$$

$$w_{ss} = \frac{4(P_w(t) - P_{w_0}).a^4}{\pi^5.D} \sum_{m=1,3,5\dots}^{\infty} \frac{(-1)^{(m-1)/2}}{m^5} \cos\left(\frac{m\pi x}{a}\right) \left(1 - \frac{\beta_a \tanh(\beta_a) + 2}{2\cosh(\beta_a)} \cosh\left(\frac{m\pi y}{a}\right) + \frac{1}{2\cosh(\beta_a)} \frac{m\pi y}{a} \sinh\left(\frac{m\pi y}{a}\right)\right) \quad (10)$$

With a and b the dimensions of the plate, and D the stiffness of the plate to bending:  $D = E.e^3/(12((1 - \nu^2)))$ ,  $\beta_a = mb\pi/(2a)$  and  $\beta_b = ma\pi/(2b)$ .

$$w_1 = -\frac{a^2}{2\pi^2 D} \sum_{m=1,3,5\dots}^{\infty} E_m \frac{(-1)^{(m-1)/2}}{m^2 \cosh(\beta_a)} \cos\left(\frac{m\pi x}{a}\right) \left(\frac{m\pi x}{a} \sinh\left(\frac{m\pi x}{a}\right) - \beta_a \tanh(\beta_a) \cosh\left(\frac{m\pi x}{a}\right)\right) \quad (11)$$

$$w_2 = -\frac{b^2}{2\pi^2 D} \sum_{m=1,3,5\dots}^{\infty} F_m \frac{(-1)^{(m-1)/2}}{m^2 \cosh(\beta_b)} \cos\left(\frac{m\pi y}{b}\right) \left(\frac{m\pi y}{b} \sinh\left(\frac{m\pi y}{b}\right) - \beta_b \tanh(\beta_b) \cosh\left(\frac{m\pi y}{b}\right)\right) \quad (12)$$

with:

$$(M_y)_{y=\pm b/2} = \sum_{m=1,3,5\dots}^{\infty} (-1)^{(m-1)/2} E_m \cos\left(\frac{m\pi x}{a}\right) \quad (13)$$

$$(M_x)_{x=\pm a/2} = \sum_{m=1,3,5\dots}^{\infty} (-1)^{(m-1)/2} F_m \cos\left(\frac{m\pi y}{b}\right) \quad (14)$$

and:

$$\left(\frac{\partial w}{\partial y}\right)_{y=\pm b/2} + \left(\frac{\partial w_1}{\partial y} + \frac{\partial w_2}{\partial x}\right)_{x=\pm a/2} = 0 \quad (15)$$

$$\left(\frac{\partial w}{\partial x}\right)_{x=\pm b/2} + \left(\frac{\partial w_1}{\partial x} + \frac{\partial w_2}{\partial y}\right)_{x=\pm a/2} = 0 \quad (16)$$

#### 4.2.2.2 Numerical value of $\alpha$ for a parallelepipedic tank

To obtain the numerical value of  $\alpha_{plate}$  such as  $\Delta P = \alpha \Delta V$  for the tank case, one needs to solve a system of partial differential equations, which requires a numerical resolution. First the variation of volume induced by an arbitrary variation of pressure of  $P_s - P_{s_0} = 1$  MPa is calculated for each plate. The obtained numerical values are presented in Table 4.

Table 4: Variation of volume authorised by the plates with respect to 1 MPa variation of pressure.

	Material	a (mm)	b (mm)	$\Delta V_{plate}$ (m <sup>3</sup> )
Tank	OMC	540	660	$7.5 \cdot 10^{-3}$
	Plexiglass	300	540	$6.9 \cdot 10^{-5}$
	Steel	300	660	$6.0 \cdot 10^{-7}$

Using (5) with  $P_s - P_{s_0} = 1$  MPa,  $\Delta V = 1.52 \cdot 10^{-2}$  m<sup>3</sup>, the obtained numerical value for the confinement parameter is:  $\alpha_{plate} = 66$  MPa.mm<sup>-3</sup> for the tank case. It is found to be closer to the calibrated one which is  $\alpha_{calib} = 150$  MPa.mm<sup>-1</sup> than the one obtained with a spherical container ( $\alpha_s = 5100$  MPa.mm<sup>-1</sup>). The ratio in the tank case between the calibrated confinement parameter and the calculated one with plates formulae is 2.27 instead of 30 with the spherical container. The bubble dynamics obtained with  $\alpha_{calib}$  is shown in Figure 6.

The prediction of the bubble dynamics obtained with  $\alpha_{plate}$  is quite satisfactory (difference between the maximum radius is 11 %, and collapse time is almost the same) knowing that the model is only an approximation of the real container response. The plates in the real container are not perfectly embedded but bolted, there are an extra reinforcement in the corners of the tank, the dimensions of the plates that effectively work in bending are not known and there are parts that are simply not modelled.

## 5 Conclusion

In the present study, the confinement in the modified Rayleigh-Plesset equation depends on two parameters :  $\Lambda$  and  $\alpha$ . The first one quantifies a correction of the Rayleigh-Plesset equation due to the finite size of the liquid domain. The second defines the confinement effect brought by the structure against the liquid expansion.

In fact, this relationship between the pressure applied to the structure and the deformation of the structure is a complex one. It depends on the container dimensions, materials, fixations, shape and on the bubble position. Obtaining this relationship would require the use of full 3D physical

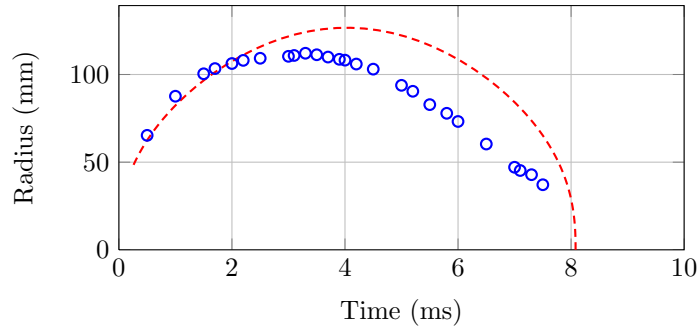


Figure 6: Radius evolution in tank test ( $\circ$ ) and predicted with confined RP in tank ( $---$ ) with  $\alpha_{plate}$ .

numerical simulations. In the present work the authors inquire on the extend to which analytical formulae permit to predict the numerical value of the confinement parameter, that is used in the Rayleigh-Plesset 1D model.

First the authors introduce a factor  $\alpha$  to obtain the simplest relationship between the pressures applied on the container and its volumic deformation. Assuming linear relationships between the internal pressure in the liquid and the volume evolution of elastic spherical containers, that are first used to represent the tested structures, the Rayleigh-Plesset equation enhanced with the confinement effect allows to describe well the radius evolution observed in the case of the pool and in the case of the water-filled tank by calibrating the proposed confinement parameter.

To the calibrated values the authors compare values calculated analytically by using an elastic formula on mono-material spherical containers with various single container materials, and with the value predicted by considering the variation of volume authorised by a multi-material parallelepipedic container. It is not possible to obtain good numerical values with the mono-material spherical container. In fact the tank walls in the tests are bending, while an elastic sphere acts as a membrane. Eventually a good estimation of the value of this parameter is obtained using plates formulae in the tank case (it is not possible to obtain this value for the pool due to the free surface). The difference between the maximal bubble radius with calibrated and calculated  $\alpha$  is 11%, knowing that several aspects such as the fixations and the bubble position effects, were not included in these formulae.

Further works are currently in progress to experimentally validate the added confinement effect to the Rayleigh-Plesset equation in 1D conditions, and to numerically assess other models and solving methods applicable to general geometries (Finite Elements, Finite Volumes, ...) to progress on the HRAM bubble dynamics understanding and prediction.



## Acknowledgement

This work has been carried out as part of the PhD thesis of the main author. The authors would like to thank the French Ministry of Defense and DGA (French Armament Procurement Directorate), for their financial support.

## References

- [1] A. Abe, M. Katayama, K. Murata, Y. Kato, and K. Tanaka. Numerical study of underwater explosions and following bubbles pulses. In *Fifteenth APS topical Conference on Shock Compression of Condensed Matter*, Kohala Coast, Hawaii, USA, June 2007.
- [2] R.E. Ball. *The fundamental of aircraft combat survivability analysis and design*. AIAA, 1985.
- [3] S.J. Bless. Fuel tank survivability for hydrodynamic ram induced by high-velocity fragments. part i experimental result and design summary. Technical Report AFFDL-TR-78-184, Part I, University of Dayton Research Institute, 1979.
- [4] E. Deletombe, J. Fabis, and J. Dupas. Vulnerability of a/c fuel tanks with respect to hydrodynamic ram pressure. interpretation of 7.62 mm experiments. In *Colloque National en Calcul des Structures (CSMA)*, 2011.
- [5] E. Deletombe, J. Fabis, J. Dupas, and J.M. Mortier. Experimental analysis of 7.62 mm hydrodynamic ram in containers. *Journal of Fluids and Structures*, 37:1–21, 2013.
- [6] J.H. McMillen. Shock wave pressure in water produced by impact of small sphere. *Physical review*, 46(9), 1945.
- [7] D. Obreschkow, P. Kobel, N. Dorsaz, A. de Bosset, C. Nicollier, and M. Farhat. Cavitation bubble dynamics inside liquid drops in microgravity. *Phys. Rev. Lett.*, 97, 2006.
- [8] H.H. Shi, M. Itoh, and T. Takami. Optical observation of the supercavitation induced by high-speed water entry. In *ASME*, volume 122, 2000.
- [9] F.S. Stepka and C.R. Morse. Preliminary investigation of catastrophic fracture of liquid-filled tanks impacted by high velocity particles. Technical Report D-1537, NASA, 1963.
- [10] S. Timoshenko and S. Woinowsky-Krieger. *Theory of plates and shells*. McGraw-Hill Book Company, 1959.
- [11] D. Varas, R. Zaera, and J. López-Puente. Numerical modelling of the hydrodynamic ram phenomenon. *International Journal of Impact Engineering*, 36:363–374, 2009.





BP 72 - 29 avenue de la Division Leclerc - 92322 CHATILLON CEDEX - Tél. : +33 1 46 73 40 40 - Fax : +33 1 46 73 41 41

[www.onera.fr](http://www.onera.fr)